Spin-coating Preparation of High Quality Mesoporous Titania Nanofilms

Ningzhong Bao,* Kazumichi Yanagisawa, Xiaohua Lu,† and Xin Feng†
Research Laboratory of Hydrothermal Chemistry, Faculty of Science, Kochi University, Kochi 780-8520
†*College of Chemical Engineering, Nanjing University of Technology, Nanjing 210009, P. R. China*

(Received October 27, 2003; CL-031020)

Highly ordered crack-free mesoporous titania nanofilms with crystalline anatase framework are obtained by spin-coating glass surface, using the very acidic solution containing ethanol, H_2O, $TiCl_4$, and P123 (Pluronic P123, an triblock copolymer $H(OCH_2CH_2)_{20}(OCH(CH_3)CH_2)_{70}(OCH_2CH_2)_{20}OH$)).

Nanocrystalline anatase is the most universal active phase in fields of photocatalysis, self-cleaning surface, and energy conversion device,[1] but it is hard to be separated from aqueous solution.[2] So, nanocrystalline anatase powders are often supported on large matrixes as films for the economic use. Mesoporous titania films also have received much attention because of large surface area.[3,4] They are usually prepared by the attractive evaporation-induced self-assembly procedure.[5] In this procedure, the preferential evaporation of a large amount of alcohol in open Petri dishes for a long time (over 2 days) concentrates the initial diluted solution containing nonvolatile surfactant and inorganic species. The formation of micelles and the organization of liquid crystal template with the simultaneous condensation of the inorganic framework to form ordered mesostructured hybrids occur at middle and last stages of the evaporation, respectively.[3–8] Because the order and structure of the mesostructures are determined by the $P123/H_2O$ molar ratio of the system of that time,[8] to quantitatively control the water content of the system is extremely important in order to obtain highly ordered mesostructured titania hybrids.[6,7] This was seldom considered in previous reports in which the water content was varied randomly by the impurities and air moisture during the uncontrollable evaporation.[3–5] As a result, the prepared hybrids are usually of low-ordered mesostructures. Recently, finely adjusting the relative moisture to prepare highly organized mesostructured hybrids was reported,[7] but both large amount of alcohol and different relative moistures corresponding to different evaporation stages are still required.

In this work, we devise a simple, repeatable, and efficient procedure to prepare crack-free nanofilm with highly ordered mesopores and crystalline anatase framework.[4] Hexagonal liquid crystal phases preorganized with $Ti(OH)_2(OEt)$ in concentrated precursor solutions containing quantitative water and a little alcohol. Nanofilm then was prepared by the spin-coating technique[9] to fast remove alcohol and "freeze" the formed mesostructure. In a typical synthesis, the homogeneous very acidic solution of 1 g P123/1 g H_2O/1.8 g $TiCl_4$/2 g ethanol was polymerized in sealed glass bottle for 5 h. Transparent nanofilm was obtained by the spin coating 2-cm^2 glass slide at 400 rpm for 4 s and then 3000 rpm for 10 s at 25 °C. Calcination of nanofilm was done in air at 400 °C for 4 h.

Low-angle powder XRD patterns of the as-synthesized mesostructured (Figure 1a) and calcined mesoporous (Figure 1b) titania nanofilms both show three resolved peaks that can be assigned to (100), (110), and (200) reflections of hexagonal structure. When compared with the as-synthesized sample the (100) peak of the calcined sample becomes wider and shifts to higher angle, owing to the shrink and crystallization of pore wall after removing the template by calcination, and other (110) and (200) peaks are also observed. These indicate the existence of ordered mesostructure within the calcined sample. The wide-angle powder XRD pattern of calcined sample (Figure 1c) is indexed as pure anatase. The broadened peaks indicate the existence of nanocrystalline anatase, with sizes of 3–4 nm estimated by applying the Scherrer formula on the (101) diffraction peak, within the pore wall. Figure 2 and corresponding inset respectively show the N_2 adsorption/desorption isotherms and BJH (Barrett–Joyner–Halenda) analysis of the desorption isotherm for the calcined sample. A clear hysteresis loop at high relative pressure is observed, which is related to the capillary condensation associated with large pore channels. The BET surface area, pore parameter, and pore volume of calcined sample are 219 m^2g^{-1}, 3.9 nm, and 0.29 cm^3g^{-1}, respectively.

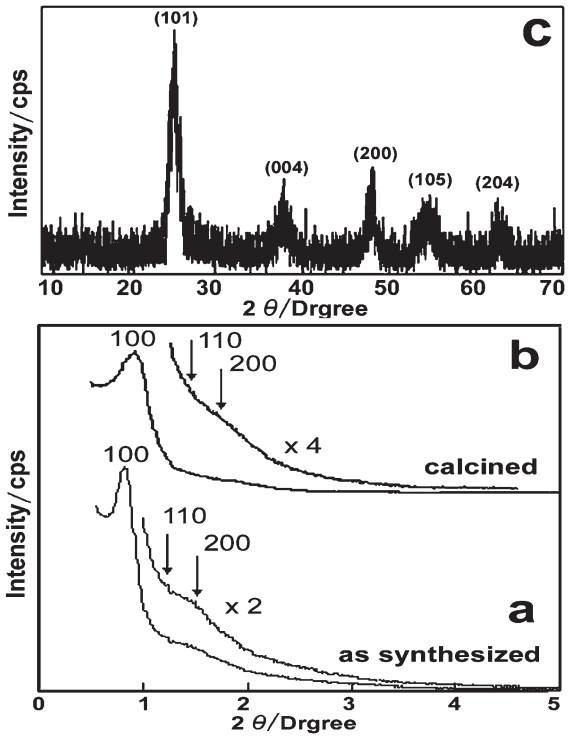

Figure 1. Low-angle XRD patterns of as-synthesized (a) and calcined (b) mesostructured titania nanofilm, and wide-angle XRD pattern (c) of calcined mesoporous titania nanofilm.

Almost all of calcined sample particles observed by TEM are of highly ordered lattice arrays (Figure 3a, b), indicating that the calcined mesoporous anatase nanofilm has uniform, large-

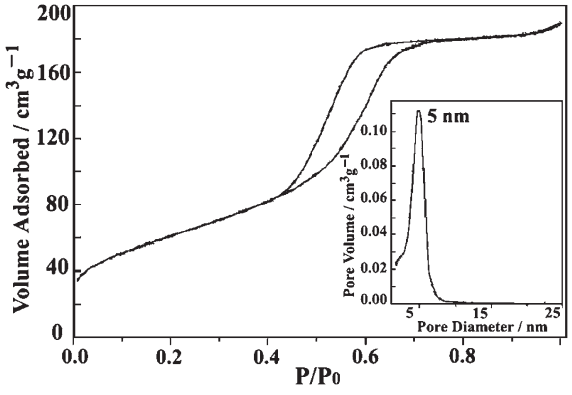

Figure 2. N_2 adsorption/desorption isotherms and BJH pore size distribution plot (inset) of calcined mesoporous titania nanofilm.

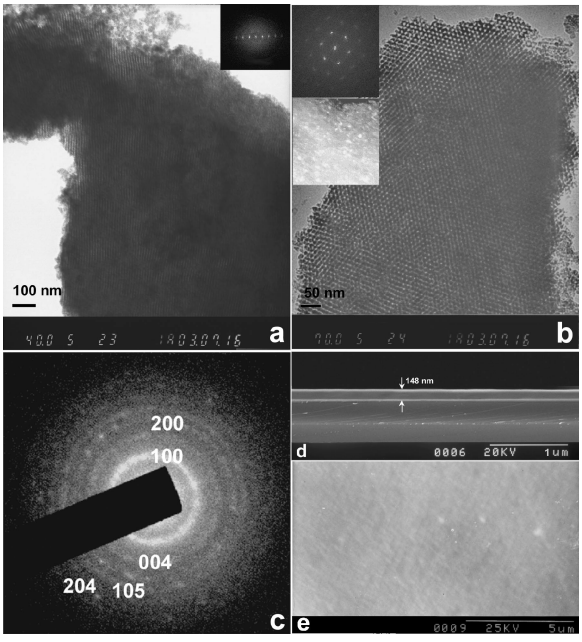

Figure 3. TEM images of calcined mesoporous titania nanofilm recorded along the (a) [110] and (b) [001] directions, respectively, with Fourier diffractograms inset. Dark-field image is also shown in the inset of (b). (c) SAED pattern obtained on image area of (b). Cross-sectional (d) and plan-view (e) SEM images of calcined mesoporous titania nanofilm.

scale, and highly ordered hexagonal mesopores. SAED (Figure 3c) recorded on mesoporous titania shows that the wall of the calcined sample comprises nanocrystalline anatase that shows characteristic electron diffraction rings, agreeing with the result of the wide-angle XRD study (Figure 1c). Bright-field and dark-field TEM imaging was used to study the distribution of these nanocrystals within the mesoporous titania. The bright spots and areas in the dark field image (the inset in Figure 3b) respectively indicate anatase nanocrystallites and pore walls. Reconciling the contrast features in Figure 3b indicates that the anatase nanocrystallites are embedded in the continuous amorphous titania matrix to form crystalline wall structures. The thickness of the nanofilm is uniform around 148 nm (Figure 3d), and can be varied from nanometer scale to micrometer scale by changing the coating speed. One representative plane-view SEM image (Figure 3e) indicates that the mesoporous anatase nanofilm is crack-free. It is possible to prepare nanofilms with large area,

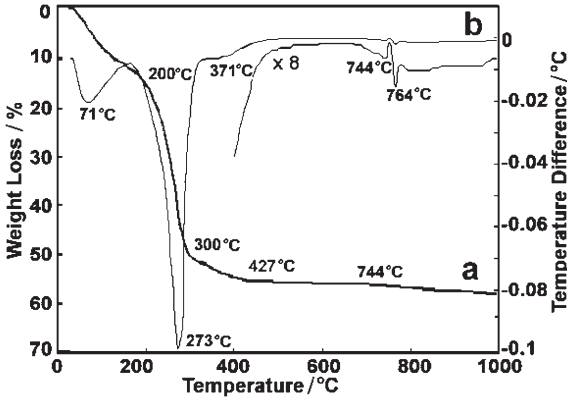

Figure 4. TGA-DTA traces of as-synthesized mesoporous titania nanofilm.

which is achieved by controlling all the amount of the prepared precursor solution, the coating technique, and the conditions.

The TGA trace of as-synthesized mesostructured titania nanofilm (Figure 4a) exhibits four obvious weight-loss steps. A first weight-loss step at $T < 220$ °C is due to the rapid decrease of alcohol, water, and HCl, corresponding to an broad endothermic peak centered at 71 °C. Two weight-loss steps at 200–300 °C and 300–427 °C respectively correspond to a strong and sharp endothermic peak centered at 273 °C and a weak and broad endothermic peak centered at 371 °C. The former one is due to the carbonization of template. The later one is due to the phase change from amorphous titania to anatase. The final small weight-loss step due to the burning of carbon occurs at $T >$ 774 °C, corresponding to an exothermic peaks at 744 °C. The endothermic peak at 764 °C is due to the phase change from anatase to rutile.

In conclusion, we obtain hexagonal mesoporous titania nanofilms with large surface area, highly ordered pore structure, and nanocrystalline anatase framework by the spin coating technique from concentrated P123–$TiCl_4$–H_2O–alcohol solution.

We thank the Outstanding Youth Fund of National Natural Science Foundation (29925616), National High-tech Research Development Program (863 Program: 2003AA333010), and Natural Science Foundation (20246002, 20236010) of China.

References

1 a) J. Retuert, R. Quijada, and V. Arias, *Chem. Mater.*, **10**, 3923 (1998). b) M. Anpo, T. Shima, S. Kodama, and Y. Kubokawa, *J. Phys. Chem.*, **91**, 4305 (1987).
2 a) R. Bauer, G. Waldner, H. Fallmann, S. Hager, M. Klare, T. Krutzler, S. Malato, and P. Maletzky, *Catal. Today*, **53**, 131 (1999). b) M. R. Hoffmann, S. T. Martin, W. Choi, and D. W. Bahnemann, *Chem. Rev.*, **95**, 69 (1995).
3 a) H. Yun, K. Miyazawa, H. Zhou, I. Honma, and M. Kuwabara, *Adv. Mater.*, **13**, 1377 (2001). b) K. L. Frindell, M. H. Bartl, A. Popitsch, and G. D. Stucky, *Angew. Chem., Int. Ed.*, **41**, 960 (2002). c) F. Bosc, A. Ayral, P. Albouy, and C. Guizard, *Chem. Mater.*, **15**, 2463 (2003). d) K. Sayama, J. Augustynski, and H. Arakawa, *Chem. Lett.*, **2002**, 994.
4 P. C. A. Alberius, K. L. Frindell, R. C. Hayward, E. J. Kramer, G. D. Stucky, and B. J. Chmelka, *Chem. Mater.*, **14**, 3284 (2002).
5 a) C. J. Brinker, Y. Lu, A. Sellinger, and H. Fan, *Adv. Mater.*, **11**, 579 (1999). b) P. Yang, D. Zhao, D. I. Margolese, B. F. Chmelka, and G. D. Stucky, *Chem. Mater.*, **11**, 2813 (1999). c) P. Yang, D. Zhao, D. I. Margolese, B. F. Chmelka, and G. D. Stucky, *Nature*, **396**, 152 (1998).
6 E. L. Crepaldi, G. J. Soler-Illia, D. Grosso, F. Cagnol, F. Ribot, and C. Sanchez, *J. Am. Chem. Soc.*, **125**, 9770 (2003).
7 T. Katou, D. Lu, J. N. Kondo, and K. Domen, *J. Mater. Chem.*, **12**, 1480 (2002).
8 P. Alexandridis, J. F. Holzwarth, and T. A. Hatton, *Macromolecules*, **27**, 2414 (1994).
9 a) M. Ogawa, *Chem. Commun.*, **1996**, 1149. b) N. Nishiyama, S. Tanaka, Y. Egashira, Y. Oku, and K. Ueyama, *Chem. Mater.*, **14**, 4229 (2002).

Published on the web (Advance View) February 23, 2004; DOI 10.1246/cl.2004.346